

## Zenithal gliding of the easy axis of a nematic liquid crystal

Stéphane Joly,<sup>1</sup> Krassimira Antonova,<sup>2</sup> Philippe Martinot-Lagarde,<sup>3</sup> and Ivan Dozov<sup>1</sup>

<sup>1</sup>*Nemoptic, 1 rue Guynemer, 78114 Magny les Hameaux, France*

<sup>2</sup>*Institute of Solid State Physics, Bulgarian Academy of Sciences, 72 Boulevard Tsarigradsko Chaussee, 1784 Sofia, Bulgaria*

<sup>3</sup>*Laboratoire de Physique des Solides, Université Paris-Sud, Bâtiment 510, 91405 Orsay cedex, France*

(Received 2 June 2004; published 19 November 2004)

We present experimental evidence of zenithal gliding of the nematic easy axis on a polyimide surface. The reorientation dynamics of the easy axis under external torque, and its relaxation, are extremely slow processes which cannot be described by a single exponential time. They show similarities with aging phenomena previously encountered in glassy systems. At last, the adsorption-desorption-readsorption process which empirically justifies the azimuthal easy axis gliding may also explain our observations.

DOI: 10.1103/PhysRevE.70.050701

PACS number(s): 61.30.Hn

One of the main issues in liquid-crystal (LC) displays is the control of the anchoring on the substrates. A change in time of the anchoring directions leads to a decrease of the optical contrast and/or the formation of shadow images, even a change of the thresholds in LC devices [1,2]. Anchoring refers to the property of the substrate to align the nematic on its surface. For constant nematic order parameter, this local average orientation of the molecules is fully characterized by the surface director  $\mathbf{n}_s = (\sin \theta_s \cos \varphi_s, \sin \theta_s \sin \varphi_s, \cos \theta_s)$ , where  $\theta_s$  is the zenithal (polar) angle and  $\varphi_s$  the azimuthal angle (Fig. 1). The easy axis  $\mathbf{e}$  is the preferred orientation of  $\mathbf{n}_s$  when it is not submitted to any external torque. It corresponds to a minimum of the anisotropic part of the surface energy  $G_s(\mathbf{n}_s, \mathbf{e})$  also called anchoring energy [3]. To a first approximation, the zenithal and azimuthal parts of the anchoring energy are not correlated:  $G_s(\mathbf{n}_s, \mathbf{e}) = G_z(\mathbf{n}_s, \mathbf{e}) + G_a(\mathbf{n}_s, \mathbf{e})$ . For infinite anchoring energy,  $\mathbf{n}_s$  stays parallel to  $\mathbf{e}$  independently of the torque. For weak anchoring energy,  $\mathbf{n}_s$  deviates from  $\mathbf{e}$  under applied torque. This process is reversible—upon torque removal  $\mathbf{n}_s$  relaxes back to  $\mathbf{e}$  within a few milliseconds.

Under strong torque applied for a long enough time, the easy axis itself can slowly rotate [4,5]. This so called easy axis “gliding” has been reported for lyotropic [6] and thermotropic [7] LC with weak azimuthal anchoring. The gliding is related to the anchoring memory [8]—on most substrates some mesogen molecules are adsorbed, keeping the memory of the interface state at the first contact with the nematic. The adsorbed strongly anisotropic layer aligns  $\mathbf{n}_s$  along the initial easy axis direction. The memory-induced anchoring can be strong and for isotropic substrates (e.g., bare glass) is the only source of azimuthal anchoring energy. At long term, the memorized easy axis can glide under external torques by desorption-readsorption processes, with step-by-step reorientation of the adsorbed molecules. This gliding is slow (time scale from a few minutes to a few months) and partially irreversible.

Here we present experimental evidence for a zenithal gliding of the easy axis of a nematic, strongly anchored on a rubbed polyimide. After a few hours under electric field we observe an important pretilt variation (about  $2^\circ$ ), partially reversible. In the framework of a simple phenomenological

model we describe the gliding as a viscoelastic process and we discuss its possible microscopic origins.

Our thin cell ( $d=1.5 \mu\text{m}$ ) filled with 4,4-pentylcyanobiphenyl (5CB) is placed in a controlled heating stage at  $20^\circ\text{C}$ . The two substrates (Fig. 1) have different anchoring layers deposited on indium-tin-oxide (ITO) electrodes. The plate 1 is spin coated with the polyimide Nissan SE-3510, giving, after rubbing, a strong anchoring (zenithal extrapolation length [9]  $L_z < 20 \text{ nm}$ ) and relatively high pretilt ( $\psi = \pi/2 - \alpha = 6.7^\circ$ ; see Fig. 1). On plate 2, a 45-nm-thick SiO film evaporated under  $60^\circ$  oblique incidence gives a planar ( $\psi_2 = 0$ ) alignment and strong anchoring ( $L_z < 15 \text{ nm}$ ) for 5CB. Without field, or under electric field  $\mathbf{E} \parallel \mathbf{z}$ , the director  $\mathbf{n}(z)$  lies in the plane ( $\mathbf{xz}$ ) and the angle  $\theta(z)$  describes completely the texture (there are no azimuthal torques).

We first measure the initial value of the pretilt  $\psi_0 = \pi/2 - \alpha_0$ . Then, to create the torque, we apply an ac voltage ( $\nu = 20 \text{ kHz}$ ) of constant root-mean-square (RMS) amplitude  $U$ . After time  $t$ , the field is temporarily switched off, for less than 3 min, to measure  $\psi(t)$ . During the measurement the torque vanishes and  $\mathbf{n}_s$  relaxes to  $\mathbf{e}$ . So, what we measure is the slow reorientation of the easy axis  $\mathbf{e}$  and not the instantaneous orientation of  $\mathbf{n}_s$ .

Our technique [10] to measure the pretilt is based on a precise measurement of the total cell birefringence  $\Delta\ell$  under weak voltage, inferior to the Fréedericksz threshold  $U_f$  [11]. For  $\psi=0$ ,  $\Delta\ell$  remains constant up to  $U=U_f$ . For  $\psi \neq 0$  on one of the plates,  $\Delta\ell$  varies with  $U$ . We infer  $\psi$  from the  $\Delta\ell(U)$

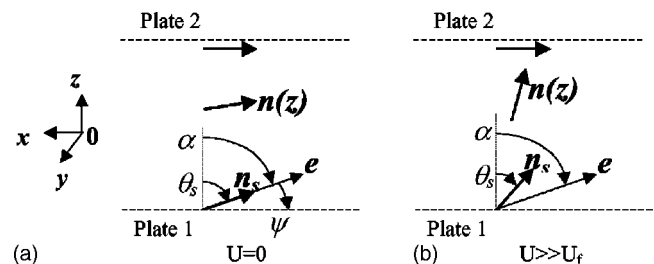


FIG. 1. Surface director  $\mathbf{n}_s$  and easy axis  $\mathbf{e}$  orientation when (a) no electric field is applied on the cell and (b) a strong electric field is applied.

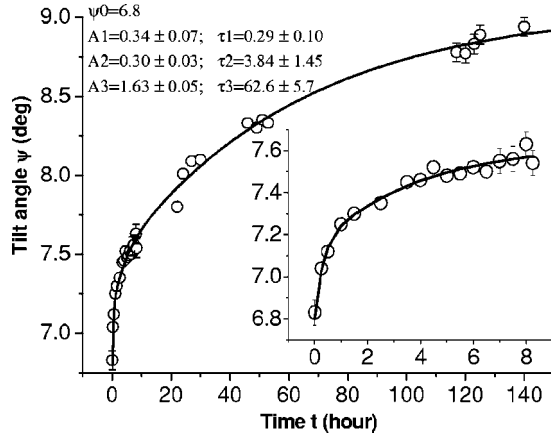


FIG. 2. Time evolution of the easy axis tilt angle under external torque created by an ac applied voltage of 5 V RMS. In the inset, details of the first 8 h. On the left-hand side are the best fit parameters with Eq. (1).

variation. Moreover, for  $U=U_f/2$  the total torque on the plate 1 vanishes [10] and  $\Delta\ell$  does not depend on the anchoring strength, but only on  $\psi$ . All measurements are performed under polarizing microscope, on a  $20 \times 20 \mu\text{m}^2$  area, with error bars [10] smaller than  $10^{-3}$  rad. The value of  $U_f = 0.79$  V is measured in the same cell, by fitting the  $\Delta\ell(U)$  curve, and takes into account the potential drop on the alignment layers.

Figure 2 presents the time evolution of the pretilt  $\psi^{on}(t)$  under field. After a cumulative time of 140 h,  $\psi$  approaches a plateau,  $\psi=8.9^\circ$ , which corresponds to a zenithal gliding  $\delta\psi=2.2^\circ$ . Different reorientation regimes are evidenced in Fig. 2 and the experimental data cannot be fitted with a single exponential time. The best fit is obtained with the function

$$\psi^{on}(t) = \psi_\infty^{on} - A_1 e^{-t/\tau_1} - A_2 e^{-t/\tau_2} - A_3 e^{-t/\tau_3}, \quad (1)$$

where  $\psi_\infty^{on}$  is the pretilt at  $t \rightarrow \infty$  and  $\tau_1^{on}=0.29$  h,  $\tau_2^{on}=3.8$  h,  $\tau_3^{on}=62$  h. These characteristic times are from 6 to 8 orders of magnitude larger than the bulk or surface director reorientation times. So, at the time scale of our experiment, the  $\mathbf{n}(z)$  and  $\mathbf{n}_s$  reaction to the field switching on and off is quasi-instantaneous, while the reorientation of  $\mathbf{e}$  is negligible during the measurement time.

After this first experiment we permanently shut off the field and we started to measure the pretilt relaxation  $\psi^{off}(t)$  (Fig. 3). After 13 days,  $\mathbf{e}$  has glided back almost to its initial position. The best fit of the experimental curve with

$$\psi^{off}(t) = \psi_0^{off} + A_1(1 - e^{-t/\tau_1}) + A_2(1 - e^{-t/\tau_2}) + A_3(1 - e^{-t/\tau_3}) \quad (2)$$

gives even longer reorientation times:  $\tau_1^{off}=0.53$  h,  $\tau_2^{off}=9.9$  h, and  $\tau_3^{off}=290$  h. The gliding back of  $\mathbf{e}$  shows that an internal torque tries to restore the initial easy axis orientation and the surface thermodynamic equilibrium.

In Fig. 4, we present the easy axis gliding as a function of the applied torque for voltages between 2 and 15 V. The cell has been left under field for 150 min, with a measure of  $\psi$

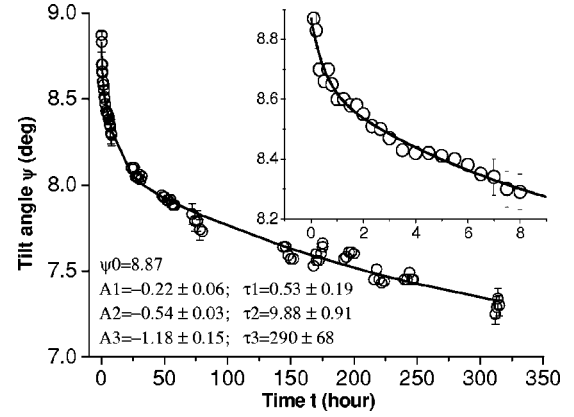


FIG. 3. Relaxation dynamics of the easy axis tilt angle. In the inset, details of the first 8 h. On the left-hand side are the best fit parameters with Eq. (2).

every 30 min. Then, the field is definitely switched off, and we continue to measure  $\psi$  periodically. The experiments were done, in increasing order of the applied voltage, on the same surface area of the cell, with typically an overnight relaxation between them. The easy axis gliding amplitude  $\delta\psi$  increases slightly (Fig. 4) with the applied torque, reaching a maximum around  $U=10-15$  V, when the electric torque transmitted to the surface is maximal. For higher voltages we expect a decrease of the easy axis gliding. However, experimental difficulties related with the ITO layers heating, no longer negligible at high  $U$ , prevented us from presenting reliable results (due to the ohmic heating, above 15 V we observe a transient variation of the birefringence on shutting off the field).

Our measurement technique assumes a planar opposite plate. However, a gliding may occur on that plate too during the experiment, influencing our results. Indeed, in a separate experiment on a cell made up of two planar SiO plates, after applying 5 V during 60 h, we observed a gliding  $\delta\psi_2=0.8^\circ$ . In the small pretilt approximation, the measured variation

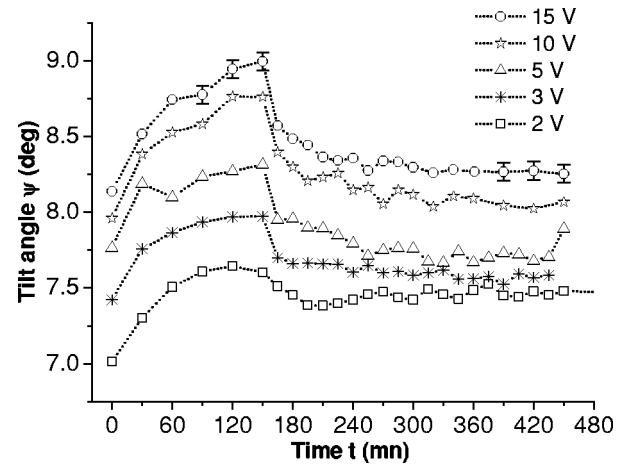


FIG. 4. Evolution of the easy axis tilt angle on the polyimide anchoring layer as a function of the voltage applied during the first 150 min. The angle values are shifted by  $0.2^\circ$  for the 3 V,  $0.4^\circ$  (5 V),  $0.6^\circ$  (10 V), and  $0.8^\circ$  (15 V) with respect to the 2-V curve.

$\Delta\ell(U_f/2) - \Delta\ell(U=0)$  is proportional to  $\psi^2/2 - \psi \delta\psi_2(\pi - 3)/\pi - \delta\psi_2^2$ . The small cross-term coefficient decreases the sensitivity to  $\delta\psi_2$ . For  $\delta\psi_2 = 0.8^\circ$  we obtain  $0.11^\circ$  uncertainty on the measured  $\psi$  values, comparable to the error bars.

Our observations can be qualitatively described in the framework of a simple visco-elastic model. The gliding back and forth implies that the easy axis  $\mathbf{e}$  can reorient under the torque applied to it by  $\mathbf{n}_s$ . Moreover,  $\mathbf{e}$  is elastically bound to its initial equilibrium orientation  $\mathbf{e}_0$  with an “anchoring energy”  $G_e(\mathbf{e}, \mathbf{e}_0)$ . The slow gliding rate shows that a large rotational viscosity  $\gamma_e$  is related to the easy axis reorientation.

Let us first consider the reorientation of the bulk director  $\mathbf{n}(z)$ , the surface one  $\mathbf{n}_s$ , and the easy axis  $\mathbf{e}$  under field (we suppose a positive dielectric anisotropy  $\epsilon_a = \epsilon_{\parallel} - \epsilon_{\perp}$ ). The electric torque applied on  $\mathbf{n}(z)$  is [9]  $\Gamma_E = -(\epsilon_0 \epsilon_a / 2) E^2 \sin 2\theta$ . In the one-constant approximation ( $K_{11} = K_{33} = K$ ) the distortion elastic torque  $\Gamma_K \cong K(\partial^2 \theta / \partial z^2)$  is opposed to  $\Gamma_E$ . The viscous torque  $\Gamma_\gamma \cong -\gamma_1(\partial \theta / \partial t)$  slows down the reorientation of  $\mathbf{n}(z)$ , where  $\gamma_1$  is the nematic rotational viscosity. The torque balance gives the characteristic bulk reorientation time  $\tau_b = \gamma_1 \xi^2 / K$ , where  $\xi = (1/E) \sqrt{K / \epsilon_0 \epsilon_a}$  is the electric-field correlation length [9]. This length may also be expressed as  $\xi = (d/\pi)(U_f/U)$ , where  $U_f = \pi \sqrt{K / \epsilon_0 \epsilon_a}$  stands for the Fréedericksz threshold [11]. For 5CB [12] at  $T = 20^\circ \text{C}$ ,  $\gamma_1 \cong 0.1 \text{ Pa s}$ ,  $K = 8 \text{ pN}$ , and for  $U = 5U_f \cong 4 \text{ V}$  and  $d = 1.5 \mu\text{m}$  we have  $\tau_b \cong 125 \mu\text{s}$ . Thus, at the time scale of the experiment, the volume is in quasiequilibrium with  $\mathbf{E}$ .

The torque transmitted to the surface [13]  $\Gamma_b \cong -(K/\xi) \sin \theta_s$  tends to align  $\mathbf{n}_s$  along  $\mathbf{E}$ . An opposed anchoring torque  $\Gamma_s = -\partial G_z / \partial \theta_s$  rotates  $\mathbf{n}_s$  toward  $\mathbf{e}$ . Here  $G_z = (W_z/2) \sin^2(\theta_s - \alpha)$  is the zenithal anchoring energy in the Rapini-Papoular approximation [14] and the anchoring strength coefficient  $W_z$  is related to the extrapolation length [9]  $L_z = K/W_z$ . At last, a surface rotational viscosity [15]  $\gamma_s$  creates a viscous torque  $\Gamma_{\gamma_s} \cong -\gamma_s(\partial \theta_s / \partial t)$ . The torque equilibrium defines the surface reorientation time  $\tau_s = \gamma_s \xi / K$ . Vilfan *et al.* [16] report  $\gamma_s / \gamma_1 \cong 100 \text{ nm}$  for 5CB on a photo-aligned layer. With this value of  $\gamma_s$ , we obtain  $\tau_s \cong 100 \mu\text{s}$  and we may suppose that  $\mathbf{n}_s$  remains always in quasiequilibrium with  $\mathbf{E}$ .

At slow time scale ( $t \gg \tau_b, \tau_s$ ) the quasistatic equilibrium of the torques [9,14], applied on  $\mathbf{n}_s$

$$\Gamma_s + \Gamma_b = \frac{K}{2L_z} \sin\{2[\alpha(t) - \theta_s(t)]\} - \frac{K}{\xi} \sin \theta_s(t) = 0, \quad (3)$$

defines the slow  $\theta_s(t)$  variation during the gliding of  $\alpha(t)$ . The source of the easy axis gliding is the anchoring torque  $-\Gamma_s$  applied by  $\mathbf{n}_s$  to  $\mathbf{e}$ . The opposed internal elastic torque is  $\Gamma_e = -(\partial G_e / \partial \alpha)$ , where  $G_e$  is the unknown surface energy of the easy axis. For small deviations  $\delta\alpha = \alpha(t) - \alpha_0$  it can be written  $G_e \cong (W_e/2) \delta\alpha^2$ , where  $W_e = K/L_e$  is the easy axis “anchoring strength” and  $L_e$  is the corresponding “extrapolation length.” Taking into account the viscous torque  $-\gamma_e(\partial\alpha/\partial t)$ , where  $\gamma_e$  is the unknown easy axis “rotational viscosity,” we obtain the torque balance equation

$$-\frac{K}{\xi} \sin \theta_s(t) - \frac{K}{2L_e} \sin 2[\alpha(t) - \alpha_0] - \gamma_e \frac{\partial\alpha}{\partial t} = 0. \quad (4)$$

The nonlinear Eqs. (3) and (4) describe the time evolution of  $\alpha$  and  $\theta_s$ . For  $L_z \ll \xi$  we can linearize the equations (for  $\pi/2 - \alpha \ll 1$ ,  $\pi/2 - \theta_s \ll 1$ ) to obtain

$$\begin{aligned} \theta_s(t) &= \alpha(t) - L_z/\xi; \quad L_e = \xi(\alpha_0 - \alpha_\infty); \\ \alpha(t) &= \alpha_\infty + (\alpha_0 - \alpha_\infty) \exp(-t/\tau_e^{om}), \end{aligned} \quad (5)$$

where  $\alpha_0 = \alpha(0)$ ,  $\alpha_\infty = \alpha(t \rightarrow \infty)$ , and  $\tau_e^{om} = \gamma_e L_e / K$  is the easy axis relaxation time under field. In a similar way, when the field is shut off we obtain an exponential relaxation of  $\alpha(t)$  back to  $\alpha_0$  with the same characteristic time  $\tau_e^{off} = \tau_e^{om}$ .

This macroscopic model is in qualitative agreement with the observed gliding behavior. From the  $U = 5 \text{ V}$  data we have  $\xi \cong 80 \text{ nm}$ ,  $\alpha_0 - \alpha_\infty \cong 0.04 \text{ rad}$ , and we obtain  $L_e \cong 3 \text{ nm}$ , i.e., the easy axis surface “elastic coefficient”  $W_e = K/L_e$  is about one order of magnitude higher than  $W_s$ . The easy axis “rotational viscosity” derived from  $\tau_e^{om}$  is  $\gamma_e \cong 2.5 \text{ Pa s m}$ ,  $10^7$  times larger than the typical surface viscosity  $\gamma_s$ . Renormalizing  $\gamma_e$  with any significant length  $L$  of our problem ( $L \leq 1 \mu\text{m}$ ), we obtain an extremely large viscosity  $\gamma_e/L$  ( $10^6$  times larger than [12]  $\gamma_1$ ). This huge viscosity has no physical meaning for the liquid crystal itself, but describes the slow processes of internal reorientation and reordering of the alignment layer and/or the nematic molecules adsorbed to it. We emphasize the large difference between the parameters ( $\gamma_e, W_e$ ) defining the slow time evolution of the easy axis and the respective variables ( $\gamma_s, W_s$ ) defining the rapid relaxation of the surface director.

Quantitatively, this macroscopic model fails to describe the complicated behavior of the gliding. Instead of a single exponential, the experimental data are best fitted with a multi-exponential (or stretched exponential) function, with strongly dispersed characteristic times (e.g.,  $\tau_3^{om} > 100\tau_1^{om}$ ). The theoretical prediction  $\tau^{om} = \tau^{off}$  fails too—the experimentally measured on and off times differ by a large factor (2–5). This discrepancy is not due to the approximate linearization of the Eqs. (3) and (4) as confirmed numerically.

The detailed microscopic discussion of the easy axis gliding is beyond the scope of the present work. However, our zenithal gliding data are quite similar to the results reported so far for the azimuthal gliding [4,5,7]. We can then suppose that the physical origins of the gliding in these two cases are the same. So far, two different mechanisms have been proposed: reorganization of the alignment layer [17,18] under external torque or desorption-readsorption [17] of a thin oriented film of nematic molecules on the substrate. The polymer reorganization seems not realistic in our case—the polyimide  $T_g$  is above  $250^\circ \text{C}$ , the chains are rigid, and not swelled by 5CB molecules. This implies low chain mobility, excluding significant reorganization of the polymer.

In the case of adsorption mechanism of the gliding, some LC molecules are physically adsorbed on the surface during the first contact with the polymer. Due to the anisotropy of the rubbed polymer and to the intrinsic nematic order (even in the isotropic phase some order subsists close to the surface

[19]) the thin adsorbed layer is well oriented. Once fixed to the surface, this layer behaves as a part of the substrate and orients  $\mathbf{n}_s$ , giving a contribution to the anchoring energy and memorizing the initial easy axis orientation  $\mathbf{e}_0$ . Due to the thermal excitation, the adsorbed layer is renewed by a slow desorption and readsorption of molecules. Without torques,  $\mathbf{n}_s$  is parallel to  $\mathbf{e}_0$  and the freshly readsorbed molecules keep in average the same orientation. Under strong torque,  $\mathbf{n}_s$  is no longer parallel to  $\mathbf{e}_0$  and the average orientation of the newly adsorbed molecules slowly rotates away from  $\mathbf{e}_0$ . The anchoring energy is now a sum of two contributions. The time-independent intrinsic anchoring energy  $G_{int}(\mathbf{n}_s, \mathbf{e}_0)$  is due to the interaction of the nematic order with the anisotropic alignment layer and to the broken symmetry at the liquid crystal/substrate interface. The adsorption contribution to the anchoring energy,  $G_{ads}[\mathbf{n}_s, \mathbf{e}_{ads}(t)]$  is time dependent due to the rotation of its easy axis  $\mathbf{e}_{ads}(t)$ . The weighted average of  $\mathbf{e}_0$  and  $\mathbf{e}_{ads}(t)$  will define the easy axis  $\mathbf{e}(t)$ . When the external field is removed, the intrinsic torque due to  $G_{int}(\mathbf{n}_s, \mathbf{e}_0)$  drags back  $\mathbf{e}(t)$  toward  $\mathbf{e}_0$ —we can identify this torque as the internal one supposed in our model. In this microscopic picture, we can qualitatively explain the extremely high value of

the easy axis viscosity—the desorption rate is slow and at each readsorption event the rotation of the easy axis is infinitesimal.

Our observations confirm for the zenithal case the main features of the easy axis gliding already reported in azimuthal geometry—the strong gliding under torque [5], the partial gliding back in the case of strong substrate anisotropy [7], the slow rate of the process, and the large dispersion of the corresponding characteristic times [4]. Multiexponential or stretched exponential function is needed to fit our data, as proposed before for the azimuthal case [4,20]. Finally, we can explain qualitatively the observed features by the readsorption mechanism first proposed for the azimuthal gliding [5]. Further work is needed to study the easy axis reorientation as a function of the anchoring strength and the temperature and hopefully to initiate the development of an accurate theoretical model.

We are thankful to Dr. D. Stoenescu and Dr. S. Lamarque, for useful discussions on the gliding data interpretation and measurement techniques.

- 
- [1] J. Nehring, A. R. Kmetz, and T. J. Scheffer, *J. Appl. Phys.* **47**, 850 (1976).
- [2] H. Hirschmann and V. Reiffenrath, in *Handbook of Liquid Crystals, Low Molecular Weight Liquid Crystals*, 1st ed., edited by D. Demus (Wiley-VCH, Weinheim, 1998), Vol. 2A, Chap. 3, p. 199.
- [3] B. Jérôme, *Rep. Prog. Phys.* **54**, 391 (1991).
- [4] S. Faetti, M. Nobili, and I. Raggi, *Eur. Phys. J. B* **11**, 445 (1999).
- [5] D. N. Stoenescu, I. Dozov, and Ph. Martinot-Lagarde, *Mol. Cryst. Liq. Cryst. Sci. Technol., Sect. A* **351**, 427 (2000).
- [6] E. A. Oliveira, A. M. Figueiredo Neto, and G. Durand, *Phys. Rev. A* **44**, R825 (1991).
- [7] V. P. Vorflusev, H. S. Kitzerow, and V. G. Chigrinov, *Appl. Phys. Lett.* **70**, 3359 (1997).
- [8] J. Cheng and G. D. Boyd, *Appl. Phys. Lett.* **35**, 444 (1979).
- [9] P. G. de Gennes and J. Prost, *The Physics of Liquid Crystals*, 2nd ed. (Oxford University Press, Oxford, 1993).
- [10] S. Lamarque-Forget, Ph. Martinot-Lagarde, and I. Dozov, *Jpn. J. Appl. Phys., Part 2* **40** L349 (2001).
- [11] E. B. Priestley, P. J. Wojtowicz, and P. Sheng, *Introduction to Liquid Crystals*, 1st ed. (Plenum, New York, 1979), Chap. 8, p. 120.
- [12] L. Pohl and U. Finkenzeller, in *Liquid Crystals Applications and Uses*, 1st ed., edited by B. Bahadur (World Scientific, Singapore, 1990), Vol. 1, Chap. 4, p. 164.
- [13] J. G. Fonseca and Y. Galerne, *Phys. Rev. E* **61**, 1550 (2000).
- [14] A. Rapini and M. Papoular, *J. Phys. (Paris), Colloq.* **30**, C4-54 (1969).
- [15] From dimensional analysis  $\gamma_s = \gamma \cdot L$ , where  $L$  is a characteristic microscopic length and  $\gamma$  a dynamic viscosity with dimension Pa s. See also G. Durand, and E. G. Virga, *Phys. Rev. E* **59**, 4137 (1999).
- [16] M. Vilfan, I. Drevenšek Olenik, A. Mertelj, and M. Čopič, *Phys. Rev. E* **63**, 061709 (2001).
- [17] D. N. Stoenescu, Ph. Martinot-Lagarde, and I. Dozov, *Mol. Cryst. Liq. Cryst. Sci. Technol., Sect. A* **329**, 339 (1999).
- [18] I. Jánossy (private communications).
- [19] H. Hsiung, Th. Rasing, and Y. R. Shen, *Phys. Rev. Lett.* **57**, 3065 (1986).
- [20] Our data are well fitted by a stretched exponential, but the physical meaning of this fit is doubtful since the error bars on the characteristic times were of the same order of magnitude and sometimes greater than the characteristic times themselves.